Mapping Out Electron-Electron Interactions at Surfaces

F. O. Schumann, J. Kirschner, and J. Berakdar

Max-Planck Institute of Microstructure Physics, Weinberg 2, 06120 Halle, Germany

(Received 19 January 2005; published 6 September 2005)

Using a high resolution coincidence technique, we measured for the first time the angular and energy correlation of an electron pair emitted from the valence band of a single crystal upon the impact of an electron with a specified momentum. We observe a hole in the measured two-particle correlation function when the two excited electrons have comparable momentum vectors, a fact traced back to exchange and repulsion among the electrons. We find the hole is not isotropic, has a finite extension, and is strongly suppressed when decoherence is operating.

DOI: 10.1103/PhysRevLett.95.117601 PACS numbers: 79.20.Kz, 68.49.Jk

A cubic centimeter of condensed matter contains, typically, 10^{23} electrons that repel one another and are attracted by a comparable number of positively charged nuclei. Displacing one electron elicits a disturbance in the whole system. So an adequate microscopic description of all the electrons appears a desperate undertaking. Surprisingly, this system of strongly interacting charged particles can be recast into a simpler one, composed of weakly or even noninteracting quasiparticles [1], while still capturing the basic physics of a variety of materials. In the condensed phase bare electrons are screened or dressed with a cloud of positive charge, and this composite object is called a quasiparticle [1–3]. If the Coulomb interactions among the valence electrons are not sufficiently screened, the quasiparticle concept is not viable and a number of electronic correlation-induced phenomena emerge. Prominent examples are high temperature superconductivity in cuprates [4] and the colossal magnetoresistance materials [5]. Thus, it is of a fundamental importance to develop a technique capable of exploring the details of the electron-electron interaction in a given sample. Present day experiments such as single photoelectron emission [6] and electron energy loss spectroscopy [7] trace the influence of electronic correlation as modifications and subsidiary structures superimposed on the single particle spectrum [8]. As pointed out by Wigner [9], in condensed matter the hallmark of the electron-electron Coulomb repulsion is a ''hole'' in the pair correlation function (the Coulomb or correlation hole) when the two electrons approach each other. Slater also indicated [10,11] that, due to Pauli's principle, exchange effects result additionally in a reduced magnitude of the pair correlation function (the exchange or the Fermi hole) when the two electrons possess equal spin projections and equal momenta. This theoretical concept of the pair exchange and correlation is at the heart of past and current developments in quantum theories for describing and predicting reliably the behavior of matter [2,3,12–14]. Over the past 60 years numerous theoretical studies explored various aspects of the exchange-correlation (xc) hole in the condensed phase [15–21], yet an experimental realization remained beyond reach. To access information on the electron-electron interaction, one focuses ideally on an electron pair in the system and monitors the probability of finding one electron in some region in momentum space while changing in a controlled manner the momentum vector of the second electron; i.e., one determines the momentum-space pair correlation function. An experimental technique capable of addressing these issues is the $(e, 2e)$ spectroscopy in reflection [22–25]. Here we report on a novel time-of-flight coincidence setup to investigate the electron pair correlation. As sketched in Fig. 1(a), a specimen is approached by an electron generated by a pulsed electron gun with an energy, E_0, and momentum vector, $\mathbf{k}_0$, which interacts with another electron residing in the valence band. The detected electron pair energies E_1, E_2 are deduced from their flight times. So the absolute values of $|\mathbf{k}_1|$ and $|\mathbf{k}_2|$ are determined. The impact position on the resistive anode determines the direction of $\mathbf{k}_2$ within a solid angle of ~ 1 sr except for the center, which is occupied by the central collector. It is exactly this feature that constitutes the major experimental advance. The small collector in turn fixes the direction of $\mathbf{k}_1$. In this way we map out the energy and momentum dependence of the electron pair correlation. The experimental energy and momentum resolution are 0.5 eV and 0.1 Å^{-1}, respectively. As inferred from Fig. 1(b), the energy, ϵ, and the wave vector, k, of the valence electron follow from the energy and wave vector conservations, e.g.,

$$\epsilon = E_0 - (E_1 + E_2) - W, \tag{1}$$

where W is the energy difference between the vacuum level and the highest occupied level with the energy $\hat{\mu}$ [cf. Fig. 1(b)]. We have chosen LiF as a sample for the following reasons. In addition to a higher coincidence rate compared to metals, the sample remains clean if kept at $\sim$400 K. For LiF the energy W is $\sim$14 eV which ensures a good separation between the elastic peak and electrons ejected from the valence band in the time-of-flight spectrum. In Eq. (1) E_0, E_1, E_2 are controllable experimentally and can be chosen such that only one valence band electron is emitted, as done in this work.

 © 2005 The American Physical Society

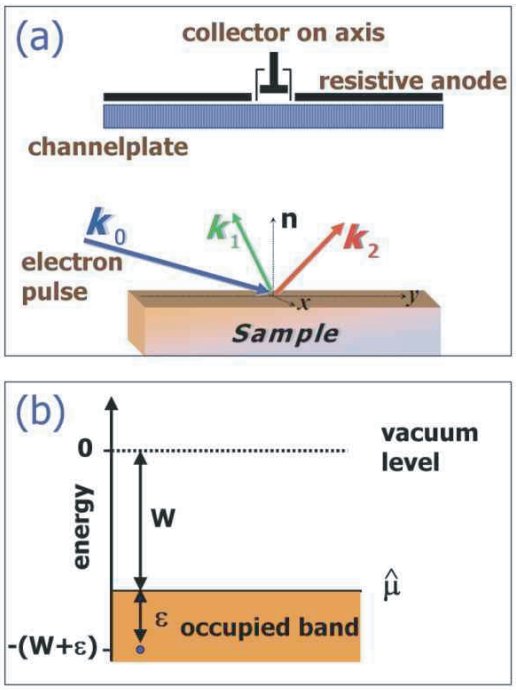

FIG. 1 (color). (a) An electron with momentum $\mathbf{k}_0$ interacts with another electron residing at the top of the valence band of the sample. Two excited electrons with momenta $\mathbf{k}_1$, $\mathbf{k}_2$ and energies E_1 and E_2 are detected in coincidence by a resistive anode and central collector. (b) Energy position of the ejected valence band electron.

A quantity of key importance for the electronic correlation in an N particle system is the reduced (two-particle) density matrix, which is given in terms of the (exact) wave function Ψ as

$$\gamma_2(x_1,x_2,x_1',x_2') = N(N-1)\int \Psi(x_1,x_2,x_3,\ldots,x_N) \times \Psi^*(x_1',x_2',x_3,\ldots,x_N)dx_3\cdots dx_N. \quad (2)$$

For fermions this equation dictates that $\gamma_2(x_1,x_2,x_1',x_2') = -\gamma_2(x_2,x_1,x_1',x_2')$. Here x_j, $j=1,\ldots,N$ stand for spin and position coordinates. The two-particle density derives from γ_2 as $\rho_2(x_1,x_2) = \gamma_2(x_1,x_2,x_1,x_2)$. Hence for fermions ρ_2 vanishes for $x_2 = x_1 = x$, i.e., $\rho_2(x,x) = 0$. On the other hand, for completely independent particles $\rho_2(x_1,x_2)$ is related to the single particle density $\rho(x)$ via $\rho_2(x_1,x_2) = \rho(x_1)\frac{N-1}{N}\rho(x_2)$. Thus, even for noninteracting (but overlapping) fermions the antisymmetry of Ψ implies a correlation among the particles that results in the existence of the (Fermi) hole in the two-particle density for $x_1 = x_2$. The Coulomb repulsion between the electrons results in additional contribution to the hole. Usually the hole is quantified by introducing the xc hole [2] $h_{xc}(x_1,x_2) = \frac{\rho_2(x_1,x_2)}{\rho(x_1)} - \rho(x_2)$ [26]. To unravel the relation of ρ_2 to the present experiment we note the following: The probability P_{if} for the transition depicted in Fig. 1 is given by [27] $P_{if} = S_{if}S_{if}^*$ where the S matrix elements are given by $S_{if} = \langle\Psi_{E_f}|\Psi_{E_i}\rangle$ and $\Psi_{E_i}(\Psi_{E_f})$ is the normalized wave function describing the system in the initial (final) state with the appropriate boundary conditions. The initial state with energy E_i describes the incident electron interacting with an electron in the valence band in the presences of all other particles in the system. The final state with energy E_f describes the two electrons that escape the sample. Within a frozen-core picture, i.e., if we assume the surrounding medium is not affected while the incident and the valence band electron are interacting and during the emission of the two electrons, we can write $\Psi_{E_i} \approx \psi_{E_i}(x_1,x_2)\chi(x_3,\ldots,x_N)$. ψ_{E_i} is the electron pair wave function in the initial state with the energy $E_i = E_0 - (\epsilon + W)$. The surrounding medium is described by χ. The reduced density matrix (2) attains then the form $\gamma_2(x_1,x_2,x_1',x_2') \approx 2\psi(x_1,x_2)\psi^*(x_1',x_2')$. Furthermore, assuming the emitted electron pair state ψ_{E_f} ($E_f = E_1 + E_2$) to be described by plane waves, we find for the measured, spin (σ_j) unresolved probability $P_{if} \propto \Sigma_{\sigma_1,\sigma_2,\sigma_1',\sigma_2'}\tilde{\psi}_{E_i}(\sigma_1\mathbf{k}_1,\sigma_2\mathbf{k}_2)\tilde{\psi}_{E_i}^*(\sigma_1'\mathbf{k}_1,\sigma_2'\mathbf{k}_2)$, where $\tilde{\psi}_{E_i}$ is the double Fourier transform of ψ_{E_i}. Hence what is measured in our experiment is the spin-averaged diagonal elements of the reduced density matrix in momentum space, i.e., the spin-averaged momentum-space two-particle density ρ_2. P_{if} possesses all aforementioned properties of ρ_2; in particular, P_{if} vanishes for $\mathbf{k}_1 = \mathbf{k}_2$. So we study correlation within the pair consisting of the approaching electron coupled to a valence band electron. The indistinguishability of these two electrons contributes to the xc hole through the exchange part.

We concentrate in the following on analyzing directly the measured (unnormalized) coincident probability $P_{if}(\mathbf{k}_1,\mathbf{k}_2)$, which we refer to by the intensity I. The relation between the initial-state correlation and the measured correlation features (in particular, the xc hole) is illustrated below: the pair correlation diminishes when slightly changing the initial state (by changing ϵ) while keeping the final state (i.e., $\mathbf{k}_1,\mathbf{k}_2$) unaltered. On the other hand, the spectra are hardly affected for the same initial state but different final state energy.

Figure 2 shows the energy correlation in the measured electron pair coincidence intensity, $I(E_1,E_2)$ with the direction of $\mathbf{k}_1$ fixed. Because of their low energies entailing a short escape depth, only the electrons from the first few atomic layers of the sample are involved [25,28]. Figure 2 reveals which electron energies are favored by the electron-electron interaction at surfaces. We recall that the electron-electron scattering in free space is governed by the form factor of the Coulomb potential that behaves as $|\mathbf{k}_1 - \mathbf{k}_2|^{-2}$. That is, when a swift electron interacts with another electron the most likely outcome is one fast and one slow electron so that $|\mathbf{k}_1 - \mathbf{k}_2|^{-2}$ is maximal. Figure 2 indicates, however, a much more complex energetic dependence of the electron-electron correlation function at surfaces; theory predicts that generally the behavior shown

in Fig. 2 is determined by the surface electronic and structural properties [29]. The pair correlation is mapped out as a function of the momentum of one electron (hitting the resistive anode). The momentum of the other electron is fixed because of the small central collector (marked by the black dot in Fig. 3). The existence of the exchange and correlation-induced hole is evidenced by Figs. 3(a) and 3(b). In free space the electron-pair correlation function is dominated by the factor $2\pi\alpha[\exp(2\pi\alpha) - 1]^{-1}$ [30], where $\alpha = 1/|\mathbf{k}_1 - \mathbf{k}_2|$. In a condensed medium the surrounding charges modify decisively the properties of the electron-electron interaction. While theory cannot provide yet a general expression for $I(E_1, E_2, \mathbf{k}_1, \mathbf{k}_2)$ the experimental findings in Figs. 3(a) and 3(b) reveal hole features that are qualitatively different from those known in the free-space or in atomic species [30]. Crystal symmetry and the direction of electron momenta determine the hole shape [31]. If the momentum vector of one electron lies in a crystal high symmetry plane the hole should possess the discrete crystal symmetry. In Fig. 3(a) we cannot clearly resolve the symmetry of the fourfold sample surface due to insufficient statistics. In Fig. 3(b) we break the alignment of electron momenta with the high symmetry planes upon a 20° rotation of the sample. As evidenced by Fig. 3(a) the hole is shifted so as to surround the fixed electron (black dot), meaning that this hole is, indeed, associated with the fixed electron. A further key issue is the range of the electron-electron interaction in a given sample which is determined by the size of the hole. In free space the bare electron-electron interaction is of an infinite range and hence $\lim_{|\mathbf{k}_1-\mathbf{k}_2|\to\infty} I(E_1, E_2, \mathbf{k}_1, \mathbf{k}_2) \to 1/|\mathbf{k}_1 - \mathbf{k}_2|$. When the electron pair is immersed in an electron gas, the electron-electron interaction is screened and the xc hole shrinks. It is only for a diminishing hole (strong screening) that the material can be viewed convincingly as a collection of independent quasiparticles [2]. Hence, the present technique may serve as a powerful tool to assess the validity of theory and to trigger new conceptual developments. In this context it is instructive to compare with the [vacuum ultraviolet (VUV)] photoemission spectroscopy (PES) [6] that has been used to study a variety of correlated materials. One can utilize Eq. (1) to study specific occupied energy states in the sample, as in PES. In contrast to VUV photons, electrons can transfer momentum and hence sample's electrons with certain energy, and the wave vector can be selected and, depending on the emitted electron energies our method can be highly surface sensitive. The energy scale at which the correlation between the selected sample electron and the test charge (incident electron) can be studied is set by $E_0 - (\epsilon + W)$, which has to be larger than W. A further key finding of the present experiments is that the electron-electron interaction, as manifested in the

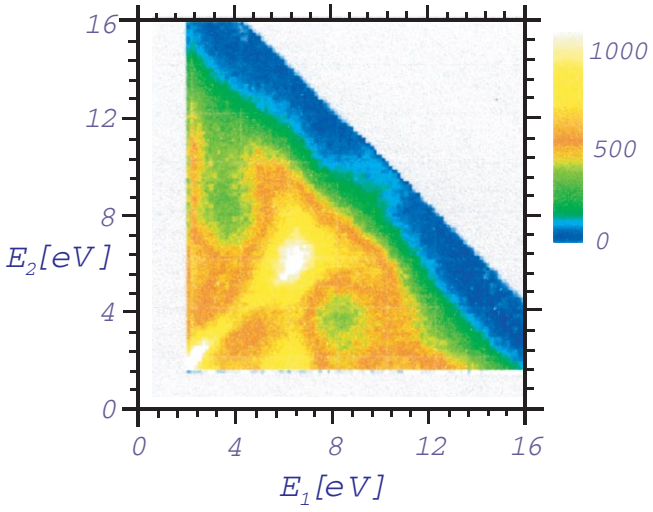

FIG. 2 (color). Energy-correlation intensity $I(E_1, E_2)$ (in arbitrary units) with the direction of $\mathbf{k}_1$ fixed. The incoming electron has an energy of 30.7 eV and the sample is a LiF(100) surface.

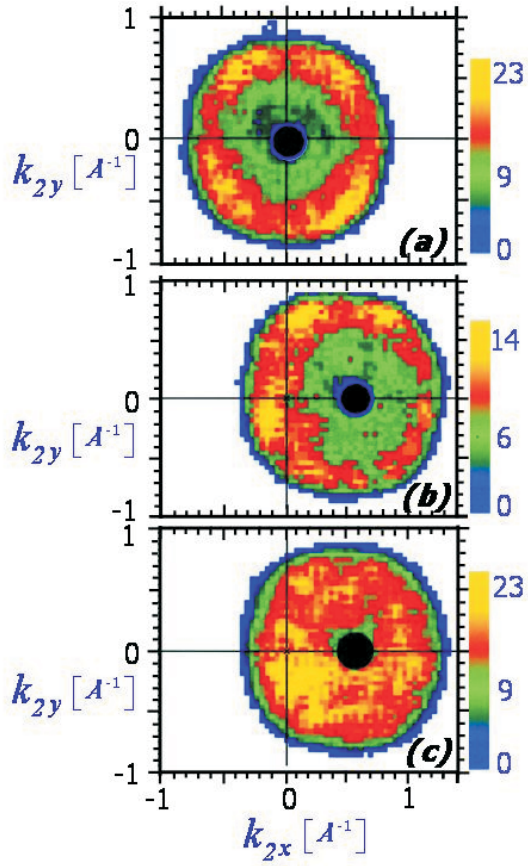

FIG. 3 (color). Intensity of the electron correlation function (in arbitrary units) versus the surface momentum components (k_{2x} and k_{2y}) of the electron with energy E_2. The energies E_1 and E_2 are 8 and 9 eV, respectively. The black dot marks the regime where the central collector is. (a) The primary energy is 30.7 eV. (b) As in (a) but the sample has been rotated by 20°. (c) As in (b), however, the impact energy is increased to 33.7 eV, i.e., the valence electron stem not from top of the valence band but from an energy band with 3 eV width below. Thus, the electron pair may undergo inelastic scattering processes resulting in decoherence of the electron waves.

xc hole is fragile to decoherence effects. To our knowledge this issue is still largely unexplored theoretically in the present context. Decoherence sets in when the correlated electron pair scatters inelastically from other surrounding electrons. We can switch off and on such mechanisms by tuning appropriately the electron energies: If E_0, E_1, and E_2 are such that the valence electron resides at the highest occupied level $\hat{\mu}$, i.e., if $\epsilon = 0$ [cf. Fig. 1(b)] the electron pair does not inelastically scatter from other particles, for such a scattering entails an energy loss of the electron pair and hence a violation of the energy conservation in Eq. (1). Electron wave coherence is not affected by elastic scattering. On the other hand, as inferred from Fig. 1(b), keeping the electron pair energies E_1 and E_2 fixed and increasing E_0 we access, in addition to the state with the energy $\epsilon = E_0 - (E_1 + E_2) - W$, a band of occupied electronic states lying between $\hat{\mu}$ and ϵ. An electron pair originating from this band has in the solid the excess energy $E_1 + E_2 + \delta$. Because of inelastic scattering from the occupied levels above ϵ, the electron pair loses the energy δ and arrives at the detector with the energies E_1 and E_2. These scattering events, whose amount can be tuned by changing δ, randomize the phase of the electron waves and eventually lead to a loss of correlation within the pair. This situation is illustrated in Fig. 3(c) for which the energies E_1, E_2 are kept fixed to be the same as in Fig. 3(a). When the primary energy E_0 is increased by $\delta = 3$ eV, the decoherence channel opens, and a complete loss of correlation within the pair is observed. Consequently, the xc hole diminishes; i.e., two incoherent electrons approach each other much closer than in situations where decoherence is suppressed and the correlation hole is fully developed [cf. Fig. 3(a)]. This finding is of key importance for the potential use of correlated electron pairs in solids for quantum information processing, as discussed in Ref. [32], for such applications require coherence within the pair. We find in this study that coherent electron pairs are only those that have the energy $E_0 - W$, i.e., where one electron originates from the valence band maximum. A realistic theoretical description of the presented experimental results, especially including the issue of decoherence is currently beyond the capabilities of existing theories. It is, however, evident that the present novel technique can serve as a probe for the nature of the electron-electron interaction in modern materials, in particular, as many of those, such as high temperature superconductors, are strongly influenced by the correlated motion of the electrons. A future implementation of a spin-polarized electron will allow the study of spin correlation of magnetic surfaces. In particular, as the electron pair interaction in metals is screened on the scale of few lattice constants the present technique holds the promise of providing information on the short-range order of the spin projections.

[1] L. D. Landau, Sov. Phys. JETP **3**, 920 (1957).
[2] P. Fulde, *Electron Correlations in Molecules and Solids*, Springer Series in Solid State Sciences Vol. 100 (Springer, Berlin, 1993).
[3] G. D. Mahan, *Many-Particle Physics* (Plenum, New York, 2000), 3rd ed.
[4] R. W. Hill, C. Proust, L. Taillefer, P. Fournier, and R. L. Greene, Nature (London) **414**, 711 (2001).
[5] M. Uehara, S. Mori, C. H. Chen, and S. W. Cheong, Nature (London) **399**, 560 (1999).
[6] *Solid-State Photoemission and Related Methods: Theory and Experiment*, edited by W. Schattke and M. A. van Hove (Wiley-VCH, Weinheim, 2003).
[7] H. Ibach and D. L. Mills, *Electron Energy Loss Spectroscopy and Surface Vibrations* (Academic Press, New York, 1982).
[8] R. Neudert *et al.*, Phys. Rev. Lett. **81**, 657 (1998).
[9] E. Wigner, Trans. Faraday Soc. **34**, 678 (1938).
[10] J. C. Slater, *Introduction to Chemical Physics* (McGraw-Hill, New York, 1939).
[11] J. C. Slater, Phys. Rev. **81**, 385 (1951).
[12] R. G. Parr and W. Yang, *Density Functional Theory of Atoms and Molecules* (Oxford University Press, New York, 1989).
[13] A. Gonis *et al.*, Phys. Rev. Lett. **77**, 2981 (1996).
[14] P. Ziesche, Int. J. Quantum Chem. **60**, 1361 (1996); Phys. Lett. A **195**, 213 (1994).
[15] M. Nekovee, W. M. C. Foulkes, and R. J. Needs, Phys. Rev. Lett. **87**, 036401 (2001).
[16] J. P. Perdew, K. Burke, and Y. Wang, Phys. Rev. B **54**, 16 533 (1996).
[17] P. H. Acioli and D. M. Ceperley, Phys. Rev. B **54**, 17 199 (1996).
[18] W. E. Pickett and J. Q. Broughton, Phys. Rev. B **48**, 14 859 (1993).
[19] J. P. Perdew *et al.*, Phys. Rev. B **46**, 6671 (1992).
[20] J. E. Inglesfield and J. D. Moore, Solid State Commun. **26**, 867 (1978).
[21] O. Gunnarsson and B. I. Lundqvist, Phys. Rev. B **13**, 4274 (1976).
[22] J. Kirschner, O. M. Artamonov, and S. N. Samarin, Phys. Rev. Lett. **75**, 2424 (1995).
[23] S. Iacobucci, L. Marassi, R. Camilloni, S. Nannarone, and G. Stefani, Phys. Rev. B **51**, R10 252 (1995).
[24] S. N. Samarin *et al.*, Rev. Sci. Instrum. **74**, 1274 (2003).
[25] A. Morozov, J. Berakdar, S. N. Samarin, F. U. Hillebrecht, and J. Kirschner, Phys. Rev. B **65**, 104425 (2002).
[26] The pair correlation function g is defined as $g(x_1, x_2) = h_{xc}(x_1, x_2)/\rho(x_2) + 1 = \rho_2(x_1, x_2)/[\rho(x_1)\rho(x_2)]$.
[27] J. Berakdar, *Concepts of Highly Excited Electronic Systems* (Wiley-VCH, Weinheim, 2003), p. 189.
[28] A. Liscio *et al.*, J. Electron Spectrosc. Relat. Phenom. **137–40**, 505 (2004).
[29] J. Berakdar, H. Gollisch, and R. Feder, Solid State Commun. **112**, 587 (1999).
[30] H. A. Bethe and E. Salpeter, *Quantum Mechanics of One- and Two-Electron Atoms* (Plenum, New York, 1977).
[31] N. Fominykh, J. Berakdar, J. Henk, and P. Bruno, Phys. Rev. Lett. **89**, 086402 (2002).
[32] D. S. Saraga, B. L. Altshuler, D. Loss, and R. M. Westervelt, Phys. Rev. Lett. **92**, 246803 (2004).